AIAA Propulsion and Energy Forum
August 24-28, 2020, VIRTUAL EVENT
AIAA Propulsion and Energy 2020 Forum

10.2514/6.2020-3622

A Predictive Hall Thruster Model Enabled by Data-Driven Closure

Benjamin A. Jorns* and Thomas A. Marks†
University of Michigan, Ann Arbor, MI, 48109

Ethan Dale ‡
University of Michigan, Ann Arbor, MI, 48109

The predictive capability of a fluid-based Hall thruster code using a data-driven closure model for anomalous electron transport is assessed. The closure model is represented as an expression for the anomalous electron collision frequency that depends analytically on the local plasma properties. This closure is incorporated into a high-fidelity multi-fluid code, which is then applied to simulate a magnetically-shielded Hall thruster operating at 300 V discharge voltage and 4.5 kW power. The uncertainties in the model parameters of the closure model are quantified through Bayesian inference, and these uncertainties are propagated forward into the predictions for the Hall thruster code. The median and 5% and 95% confidence intervals of the model predictions are compared to experimental measurements of discharge current, thrust, and ion velocity. It is found that the model predicts features qualitatively similar to the experiment including low-frequency oscillations in the discharge current and the periodic movement of the ion acceleration zone. However, the simulated frequencies and amplitudes of oscillations are higher than measured in the experiment and the median predicted performance metrics are 15-20% lower. These results are discussed in the context of the physical significance and limitations of the data-driven approach to closure.

Nomenclature

B_0	=	Applied magnetic field
c_s	=	Ion sound speed
E	=	Applied electric field
I_D	=	Discharge current
$je(z)$	=	Electron current density parallel to applied electric field
jde	=	Electron current density in E $\times$ B direction.
L	=	Discharge chamber length
m_e	=	Electron mass
n_e	=	Electron density
ν_e	=	Total electron collision frequency
$\nu_{e(c)}$	=	Classical electron collision frequency
ν_{AN}	=	Anomalous electron collision frequency
ω_{ce}	=	Electron cyclotron frequency
$P(\Theta;\sigma\|d)$	=	Posterior distribution function
$P(d\|\Theta;\sigma)$	=	Likelihood function
$P(\Theta;\sigma)$	=	Prior distribution function
$P(d)$	=	Evidence
R_{CL}	=	Radial location of channel centerline
q	=	Fundamental charge
σ	=	Measurement uncertainty for anomlaous electron collision frequency
T_e	=	Electron temperature (eV)

*Assistant Professor, Department of Aerospace Engineering, AIAA Senior Member
†PhD. Candidate, Department of Aerospace Engineering, AIAA Student Member
‡Postdoctoral Fellow, Department of Aerospace Engineering, AIAA Member

Θ	=	Model parameters for data-driven closure model
u_i	=	Ion drift speed in axial direction
v_{de}	=	Electron drift speed in Hall direct
z^*	=	Axial location where closure model is replaced with Bohm scaling

I. Introduction

The Hall effect thruster is an attractive technology for in-space propulsion, balancing a moderate thrust density with high specific impulse (> 2000s). These advantages have led to the widespread operational use of these devices for applications ranging from geocentric orbit raising to station keeping. Despite the growing maturity of this technology, however, there are a number of outstanding challenges related to their future development. These include open questions about the fidelity of ground tests for representing on-orbit performance [1–3] and how to perform lifetime assessments for higher-power, longer duration operation [4]. This latter question is particularly pressing in light of two upcoming deep space missions that baseline Hall thrusters [5, 6]. Many of these challenges could be addressed in part through analysis, i.e. the use of high fidelity predictive numerical models. However, to date, the predictive capability of Hall thruster models has been limited.

This limited predictive capability of Hall thruster models stems from a lack of understanding of key physical processes that govern Hall thruster operation [7, 8]. In order to yield simulated results that can be leveraged for addressing operational challenges, Hall thruster models that are used for technology development employ a fluid or hybrid-fluid approximation for the plasma [9]. While there are well-established classical fluid equations for low temperature plasmas like that found in the Hall thruster, it has been shown experimentally that not all of these classical equations apply to this device. Most notably, the cross-field electron current is orders of magnitude higher than can be explained by classical transport theory. Indeed, while the mechanisms that govern this transport remain poorly understood, several theories suggest that it is kinetic—not fluid— in nature (c.f. [7, 10]).

Faced with this limitation, the electron transport in fluid-based Hall thruster codes is typically represented with an ad-hoc transport coefficient—either in the form of an anomalous collision frequency or mobility. This invites a closure problem. By introducing a new free parameter, the governing set of equations is opened and cannot be solved. It is therefore common practice to close the equations by prescribing fixed values of this coefficient at each location of the simulated domain. These values are then adjusted until the code yields predictions consistent with experimental measurements [8, 11]. In this way, numerical models have been able to match experiment with a high-degree accuracy. This approach similarly has been applied to guide physics-based investigations (c.f. [12–19]) and to complement design and qualification efforts [20–23]. With that said, despite the high utility of this approach to numerical modeling, it has a limited predictive capability. There must first be experimental measurements of an actual system to infer the values for the transport coefficients.

In an effort to overcome this challenge, there have been a number of attempts to date to close the governing fluid equations for the Hall thruster. These approaches primarily have been physics-based: a process is hypothesized to explain the electron dynamics, and this is then used to guide the derivation of a simplified form for the transport coefficient [16, 24–33]. While these previous efforts have the advantage of being rooted in physical intuition about the system, practically, their ability to predict the experimentally-measured transport in the thruster has been limited. As an alternative, we recently explored in Ref. [10] a data-driven approach to the problem of closure in Hall thrusters. By using datasets of the experimentally-inferred values of electron anomalous collision frequency over a wide range of parameter space, we were able to employ symbolic regression to identify new closure models for this transport coefficient. We showed that these models exhibited improved predictive capability for the transport coefficient as compared to previous physics-based models. With that said, we have yet to self-consistently incorporate these data-driven closures into a full Hall thruster simulation. This is a critical step for demonstrating the predictive capability of the data-driven approach.

With this in mind, the goals of this work are to implement one of our data-driven models for the anomalous collision frequency into a Hall thruster code, to quantify our confidence in the model predictions, and to compare the model predictions to experimental measurement. To this end, this paper is organized in the following way. In the first section, we review the problem of anomalous transport, introduce a data-driven closure model for this transport, discuss the application of Bayesian inference to quantify uncertainty in this closure model, and overview the Hall thruster code we used for this study. In the second section, we present results that include uncertainty quantification in the closure model parameters as well as predictions from the thruster code. In the third and final section, we discuss the physical implications and limitations of our results.

II. Approach to modeling

We overview in this section the key elements for our approach to predictive Hall thruster modeling. We begin with a description of the closure problem as it relates to an anomalous collision frequency. We then present a data-driven model for this collision frequency and a rigorous method for determining its model parameters. We conclude with an overview of the modeling framework into which we incorporated our data-driven closure model.

A. Anomalous collision frequency in Hall thrusters and the problem of closure

Fig. 1 shows a canonical geometry and coordinate convention for a Hall effect thruster. These axisymmetric devices are characterized by an axial electric field and radial magnetic field. The magnetic field magnitude is tailored such that only the electrons are magnetized and subsequently trapped in a closed, E×B current, j_{de}, where they serve to ionize the propellant and maintain quasineutrality. The heavier, unmagnetized ions are accelerated out of the thruster by the applied electric field. Ideally, while no electrons are able to cross the magnetic field in the axial direction, in practice there is a finite electron current density. This is typically represented in Hall thruster fluid-based models in terms of an Ohm's law[11, 34]:

$$j_{e(z)} = \frac{m_e n_e \nu_e}{B_0^2}\left(\frac{1}{q n_e}\frac{\partial n_e T_e}{\partial z} + E\right), \tag{1}$$

where E denotes the local electric field, $j_{e(z)}$ is the electron current density in the direction of the electric field, B_0 is the magnitude of the applied magnetic field, q is fundamental charge, n_e is the electron density, T_e is the electron temperature expressed in electron volts, and ν_e denotes an effective electron collision frequency. As Eq. 1 shows, as the electron collision frequency increases, more electron current is allowed to flow across field lines.

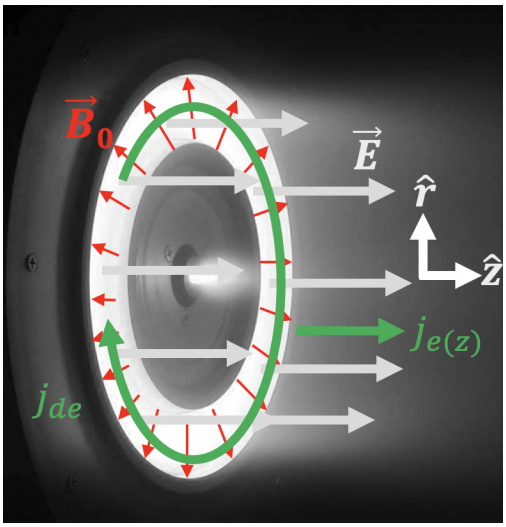

Fig. 1 Canonical geometry and coordinate convention for the Hall thruster showing applied fields and resulting electron drifts.

There are known classical expressions for the electron collision frequency, $\nu_{e(c)}$ that are based on the assumption that the electron dynamics are dominated by interspecies collisions [34]. However, when these expressions are employed in Eq. 1, it is found that predictions for electron current are orders of magnitude lower than observed in experiment. It therefore is common practice to introduce an ad-hoc or anomalous collision frequency, ν_{AN}, such that

$$\nu_e = \nu_{e(c)} + \nu_{AN}. \tag{2}$$

This anomalous collision frequency can be adjusted to raise the effective electron current to match experimental measurements.

While the introduction of the anomalous collision frequency into the classical fluid equations allows for simulations to better represent the measured electron transport in these devices, in practice, this new variable leads to a closure problem. The number of unknowns exceeds the number of equations. To close the governing equations and therefore

arrive at a self-consistent model for the thruster, it is necessary to find an additional governing equation—a closure model—for this new collision frequency that relates back to the parameters solved for in the original fluid formulation, i.e. $\nu_{AN}(T_e, E, ...)$.

B. Data-driven closure model for anomalous collision frequency

We recently explored in Ref. [10] a data-driven method to find a closure model for anomalous collision frequency. This was based on regressing datasets from previously measured values of ν_{AN} as a function of local plasma properties, e.g. temperature, density, and local drift speeds. We employed a symbolic genetic algorithm to search functional space for different closure models that fit the data. We in turn were able to show that the resulting closures yielded predictions for the dependence of the measured collision frequency on plasma properties with an order of magnitude improvement in goodness of fit over some previous physics-based closure models. We similarly demonstrated that the data-driven models were extensible—they could be used to match new datasets beyond those that were used to train them.

While this approach yielded a family of possible analytical models that could fit the data, we consider here as a case study only one of the results (Data-driven model I in Ref. [10]):

$$\nu_{AN}(c_s, u_i, \nu_{de}, \omega_{ce}, \Theta) = \omega_{ce}\left(c_0 + \frac{c_1 u_i}{c_2 c_s + \nu_{de}}\right), \tag{3}$$

where ω_{ce} is the electron cyclotron frequency, u_i is the local ion drift speed, c_s is the ion sound speed, and ν_{de} is the electron drift velocity in the Hall direction. We also have introduced model parameters, $\Theta = (c_0, c_1, c_2)$ that are constants. The values for these model parameters were reported in Ref. [10] as $\Theta = (-3.37 \times 10^{-2}, 2.39, 3.32)$; however, as we discuss in the following, we leave these as free parameters to be inferred in this work.

C. Bayesian inference for model calibration

The expression in Eq. 3 is a reduced fidelity approximation for the more complicated physical process that governs the anomalous transport. The need for adjustable model parameters, Θ, that must be calibrated against data is a direct consequence of the model's lower fidelity. The challenge lies in determining values for these coefficients that best represent the data but that also can describe the plasma state under multiple and varied operating conditions.

With this in mind, the model parameters can be inferred through simple linear regression, as we did in Ref. [10]. However, this approach only yields one set of parameters—the set that minimizes the residual of the error between the model and data. Choosing only one value does not reflect the inherent uncertainty in the model and data. For example, since Eq. 3 was not derived from first principles and is a fluid approximation to a kinetic process, it is possible that it is missing relevant aspects of the physics. This can be represented as uncertainty in the model parameters. Similarly, the dataset for performing the model inference is inherently sparse, and there thus is a corresponding uncertainty as to how extensible the model parameters are to new operating conditions. Both these sources of uncertainty will directly impact the predictions from Eq. 3 and by extension any thruster code that incorporates this closure.

In order to quantify the uncertainty in these coefficients, we adopt a probabilistic approach based on the method of Bayesian inference [35]. In this case, we treat the model parameters as random quantities that are described by posterior probability distributions:

$$P(\Theta; \sigma \mid d) = \frac{P(d \mid \Theta; \sigma) \cdot P(\Theta; \sigma)}{P(d)}, \tag{4}$$

where d is the experimental dataset, $P(d)$ is the Bayesian evidence, σ is a model error parameter, $P(\Theta; \sigma) = P(c_0)P(c_1)P(c_2)P(\sigma)$ is the prior probability distribution of the model parameters (assumed to be independent), and $P(d \mid \Theta; \sigma)$ is the likelihood. Physically, this expressions, which is a form of Bayes' theorem, indicates the probability that a given set of model parameters Θ is correct given the dataset, d.

The dataset we use for inference is the same training data reported in Ref. [10]. This is comprised of the inferred anomalous collision frequency as a function of local plasma properties for four different Hall thrusters and seven operating conditions:

$$\begin{aligned} d = [&\{(c_{s(1)}, u_{i(1)}, \nu_{de(1)}, \omega_{ce(1)}), \nu_{AN(1)}\}, \\ &\{(c_{s(2)}, u_{i(2)}, \nu_{de(2)}, \omega_{ce(2)}), \nu_{AN(2)}\}, \\ &\dots \\ &\{(c_{s(N)}, u_{i(N)}, \nu_{de(N)}, \omega_{ce(N)}), \nu_{AN(N)}\}], \end{aligned} \tag{5}$$

where $N = 650$ is the length of the dataset. For the likelihood, we assume a normal distribution:

$$P(d \mid \Theta; \sigma) = \prod_{j=1}^{N} \frac{1}{\sigma_j \sqrt{2\pi}} \cdot \exp\left[-\frac{1}{2}\left(\frac{\nu_{AN(j)} - \nu_{AN}(c_{s(j)}, u_{i(j)}, v_{de(j)}, \omega_{ce(j)}, \Theta)}{\sigma_j}\right)^2\right], \tag{6}$$

where $\nu_{AN(j)}$ denotes the measurement from the j^{th} element of the dataset, d, σ_j denotes experimental error in the measurement, and $\nu_{AN}(c_{s(j)}, u_{i(j)}, v_{de(j)}, \omega_{ce(j)}, \Theta)$ is the function given by Eq. 3 evaluated for the argument given by the j^{th} element of the dataset, d. Assuming the model for the anomalous collision frequency with the fit parameters Θ is correct, Eq. 6 represents the likelihood that we would measure the given dataset assuming the data is normally distributed.

For our datasets, there is no uncertainty reported and therefore no prescribed values of σ_j. We therefore have elected to treat these measurement uncertainties as model parameters that also will be inferred from Bayesian analysis. With that said, if we assumed each measurement error was an independent parameter, this would expand the dimension of the model parameter space to N, which is prohibitively large. To avoid this problem, we make an informed estimate for the form of this error based on Eq. 1. When we infer the collision frequency in the plasma, we are solving this Ohm's law using direct experimental measurements (or simulated measurements from calibrated models) of the local plasma properties. This functional relationship is given by

$$\nu_{AN} = \omega_{ce} f(E, n_e, T_e, B_0, j_{e(z)}), \tag{7}$$

where f is a non-dimensional function of the local plasma properties. We thus can relate the measurement uncertainty in the collision frequency measurement, $\delta\nu_{AN}$ to measurement uncertainties in the arguments of f:

$$\delta\nu_{AN} = \omega_{ce}\left(\left(\delta E \frac{\partial f}{\partial E}\right)^2 + \left(\delta T_e \frac{\partial f}{\partial T_e}\right)^2 + \left(\delta n_e \frac{\partial f}{\partial n_e}\right)^2 + \left(\delta j_{e(z)} \frac{\partial f}{\partial j_{e(z)}}\right)^2\right)^{1/2}, \tag{8}$$

where we have assumed there is no uncertainty in the magnetic field measurement (and thus ω_{ce}). From this result, it is evident that the uncertainty in the measured collision frequency will scale with the cyclotron frequency and the fractional error in the measured plasma properties. For simplicity of evaluation, we make the strong assumption that the parenthetical quantity in the argument of Eq. 8 is a constant, representing an average measurement error over the plasma properties. We therefore can express the variance in Eq. 6 as

$$\sigma_j = \delta\nu_{AN(j)} = c_3 \omega_{ce(j)}, \tag{9}$$

where c_3 is a constant of proportionality. Formulated in this way, c_3 becomes another effective model parameter to be inferred through inspection of the data.

The prior distributions of the model parameters, $P(\Theta; \sigma) = P(\Theta; c_3)$, in Eq. 4 reflect our prior knowledge about the probability distributions of these terms. In our case, our choice of priors is guided by the previous work in Ref. [10] that showed a best-fit value from linear regression of $\Theta = (-3.37 \times 10^{-2}, 2.39, 3.32)$. We prescribe a range of possible values for each coefficient based on this best value and assume the parameters are uniformly distributed in these ranges. Similarly, for the measurement uncertainty coefficient, we assume $0.05 < c_3 < 1$ where we have introduced a lower bound to prevent measurement uncertainty from being 0. The upperbound reflects our belief that the electrons will remain magnetized in the thruster main discharge such that the anomalous collision frequency will not exceed the cyclotron frequency. Taken together, these assumptions about the model coefficients are expressed as

$$P(c_0) = \mathcal{U}(-3 \times 10^{-1}, 3 \times 10^{-1}) \qquad P(c_1) = \mathcal{U}(0, 5) \qquad P(c_2) = \mathcal{U}(0, 5) \qquad P(c_3) = \mathcal{U}(0.05, 1). \tag{10}$$

Finally, we note that calculating the evidence term, $P(d)$ in Eq. 4 is non-trivial (and in most cases intractable). However, there are well-established sampling methods to approximate the posterior distributions of model parameters without explicitly evaluating the evidence [36]. We adopt such a sampling method in this work and subsequently leverage it to forward propagate the uncertainty in the model parameters through to the predictions from the Hall thruster code.

D. Multi-fluid Hall thruster model

We used Hall2De, a multi-fluid, two-dimensional plasma physics code to perform Hall thruster simulations with the data-driven closure. This numerical was developed by the Jet Propulsion Laboratory and has been used extensively

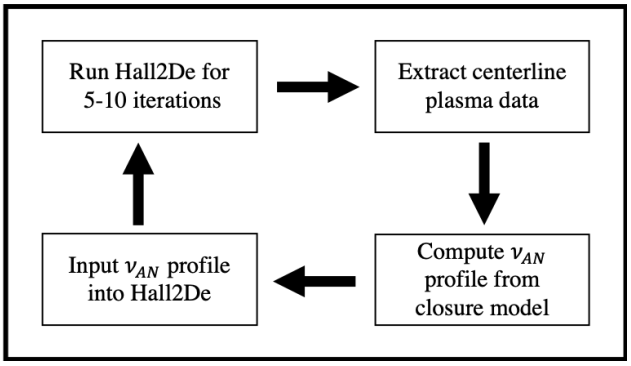

Fig. 2 Outer loop algorithm for implementing data-driven closure model with Hall2De.

to simulate several state of the art Hall thrusters [17, 20–22, 37–39]. A detailed overview of the code can be found in Ref. [11]. We describe here its salient features and underlying assumptions. Hall2De assumes an axisymmetric geometry for the thruster and employs a magnetic field aligned mesh that is defined in the radial and axial coordinates. The governing fluid equations, continuity, momentum, and energy, are solved simultaneously along this mesh for the ions and electrons in the code. The electrons, as noted above for Eq. 1 are assumed to be inertialess and therefore described an Ohm's law. Hall2De has the capability to model multiple ion species, differentiated by charge state and the location where they are born in the plasma. The discriminator for this latter featured is dictated by the electrical potential where ions are created by ionization.

Key inputs to the model include the thruster geometry and material, mass flow rate, the discharge voltage, the number of ion fluids and charge states to be modeled, magnetic field topography and strength, and the boundary conditions. The anomalous collision frequency is also treated as an input where it is prescribed as a function of axial position along the channel centerline, $\nu_{AN}(z, R_{CL})$. This frequency is then mapped to the rest of the simulated domain along magnetic field lines. Wherever a field line intersects the channel centerline of the thruster, the prescribed value of anomalous collision frequency is assigned. This same value is used along the entire magnetic field line but scaled at each location by the strength of the magnetic field. Key model outputs of Hall2De include the total discharge current, performance (thrust, efficiency, and specific impulse), and local values of the electric field and the plasma fluid properties of each species (densities, velocities, and temperatures). The code has the ability to vary the collision frequency profile automatically to achieve specified targets (e.g. a discharge current setpoint), though this option was not enabled for this work.

In order to test our closure model with Hall2De, we adopted the outer-loop approach shown in Fig. 2. We ran the code for a fixed set of time steps, M, and then exported the ion sound speed, c_s, electron azimuthal drift, v_{de}, ion drift, u_i, and electron cyclotron frequency, ω_{ce} along the channel centerline. We used these values in Eq. 3 to calculate the collision frequency profile from the closure model along channel centerline and then used this profile as a new input to Hall2De. With this new collision frequency profile, we ran the code again and repeated the process. In order to avoid non-physical results (e.g. negative collision frequencies) during this outer loop implementation, we made two additional assumptions: the anomalous collision frequency has a floor of $\nu_{AN} > 10^{-4}\omega_{ce}$, and a half channel length downstream of the magnetic field peak, denoted location z^*, we replace the closure model with the approximation $\nu_{AN}(z)/\omega_{ce}(z) = \nu_{AN}(z^*)/\omega_{ce}(z^*)$. This latter requirement is consistent with previous numerical studies that have shown the collision frequency becomes Bohm-like downstream of the acceleration zone [13].

For the results reported here, the time step we employed for Hall2De was 2×10^{-8} s. In order to ensure that we did not artificially introduce numerical oscillations with the outer loop approach, we varied randomly the number of iterations, $M = 5 - 10$, we ran the code before repeating the loop. Simulation lengths in real time were typically 3×10^{-4} s. This was sufficiently long to indicate oscillations consistent with the "breathing mode" (typically 10-20 kHz).

E. Simulated thruster

Fig. 3(a) shows the H9, a 9-kW class Hall thruster, that we simulated for this study. This device, which is described in more detail in Refs. [40–42], was developed jointly by the University of Michigan, the Jet Propulsion Laboratory, and Air Force Research Laboratory. It employs a center-mounted LaB_6 hollow cathode and a magnetic shielded topography. For this work, we modeled one operating condition, 300 V discharge voltage on xenon with a nominal power of 4.5 kW. The inputs to Hall2De (shown in tabular form in Fig. 3(b)) are based on the experimental conditions for this

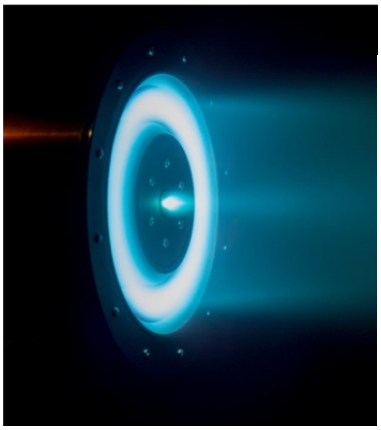

(a)

Input	Value
Anode flow rate	14.9 mg/s
Cathode flow fraction	7%
Discharge voltage	300 V
Number of ion charge states allowed	3
Number of ion fluids	2
Energy discriminator for ion fluids	250 and 40 V

(b)

Fig. 3 a) The H9 Hall thruster firing at 300 V and 4.5 kW on xenon gas. b) Input conditions to Hall2De for simulating the H9

state. The measured magnetic field of the thruster similarly was used to generate the field aligned mesh for the code. For comparison to simulation, we employ previously reported experimental measurements of the ion velocity along centerline, thrust, specific impulse, efficiency, and discharge current [42, 43]. We note here that measurements from the H9 were not included in the training data we used in Ref. [10] to arrive at Eq. 3. The use of our closure model on a thruster model for the H9 therefore is intended to be a demonstration of a predictive capability.

III. Results

We present in the following our results for parameter estimation for the closure model as well as the predictions from the Hall thruster code.

A. Model parameters

Fig. 4 shows the marginalized and joint distributions of the model parameters, (Θ, c_3), determined from Eq. 4. To generate this result, we employed a Markov Chain Monte Carlo (MCMC) method with a Metropolis Hastings algorithm to sample the posterior distribution 100,000 times [35]. For both the joint and marginalized distributions, we applied a kernel density distribution function based on the Silverman rule of thumb [44] to smooth the results. As can be seen, in all cases the marginals are approximately normal with tails well within the bounds of the priors we assumed. The joint distributions in each case exhibit a high correlation between parameters. This is represented by the elongated structures with probability contours following a narrow line with finite slope. The fact this correlation exists indicates there may a functional relationship between the fit coefficients, though exploring this relationship is beyond the scope of this work.

From the Markov Chain we employed to generate these samples, the model parameters that correspond to the maximum a posteriori probability (MAP) estimates are given by $\hat{\Theta} = (-0.045, 2.43, 3.45)$. For comparison, in our Ref. [10] where simple linear regression was applied, we found $\Theta = (-0.037, 2.39, 3.32)$. The method of Bayesian parameter estimation thus yields similar values to the previously reported best set of coefficients. As a final note, we see that the coefficient of the error term has a most probable value of $c_3 = 0.175$. In the context of the error model we proposed in Sec. II.C, this suggests $\delta\nu_{AN} = 0.175\omega_{ce}$ where $\delta\nu_{AN}$ is the uncertainty in the dataset , d, of the reported collision frequencies.

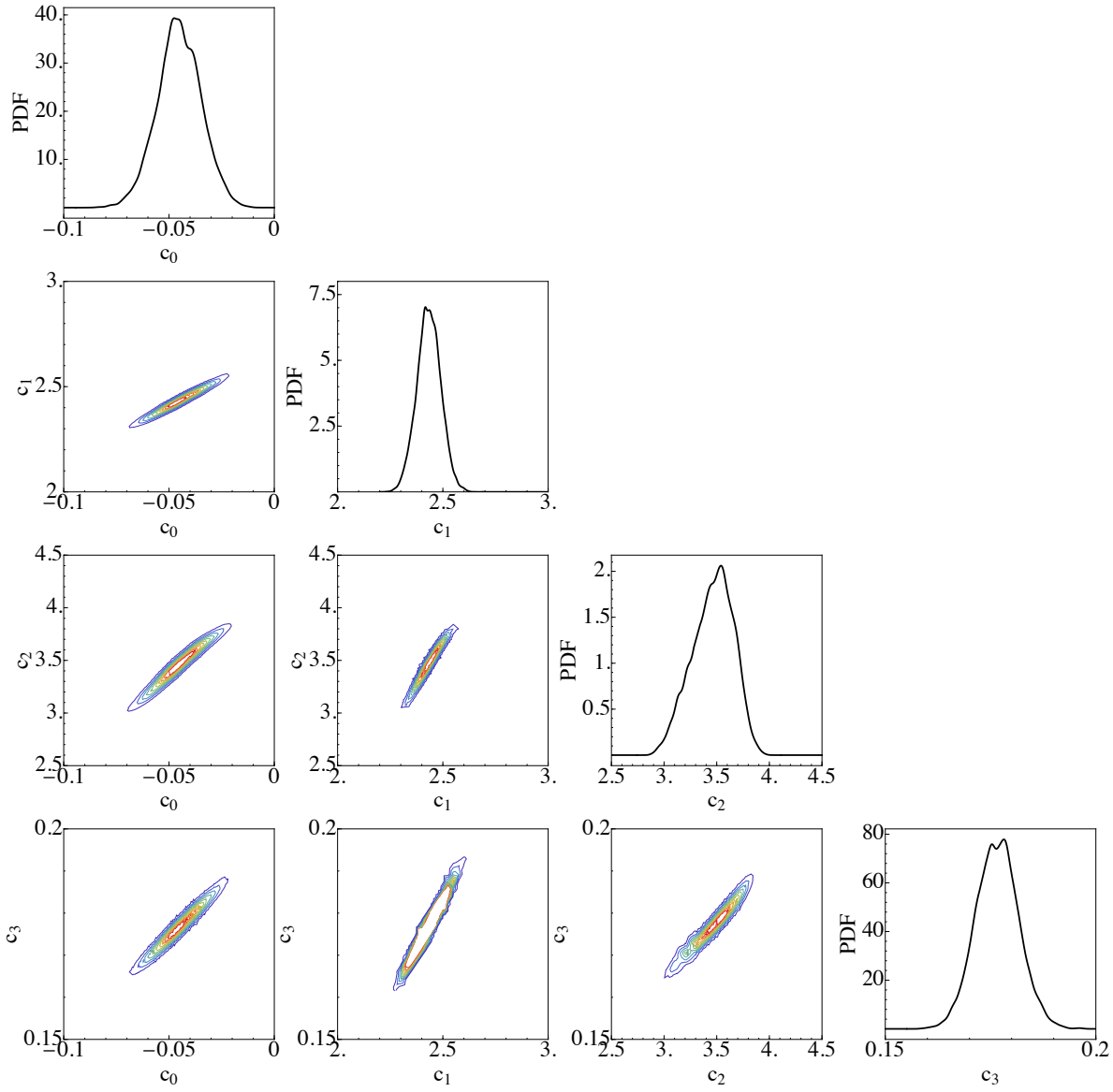

Fig. 4 Marginal and joint posterior distributions for the model parameters in Θ and c_3. Plot generated with 100,000 MCMC samples.

B. Hall thruster simulations

We consider here two cases of running Hall2De with the data-driven closure. In the first, we report the output from a single run of the code with a randomly drawn sample from the posterior distribution shown in Fig. 4. In the second case, we make a probabilistic prediction for the thruster operation by sampling multiple times from the posterior.

1. Results with single set of model parameters

We first ran the Hall2De simulation with the data-driven closure for a single set of model parameters, $\Theta = (-0.071, 2.68, 3.42)$, drawn from the posterior distribution in Fig. 4 and for a total simulated time of 0.3 ms. In the following, we compare key outputs from the model along with experimental data. To this end, we first show in Fig. 5(a) the simulated discharge current starting at 0.05 ms (after the initial transients from start up converged) and the experimentally-measured discharge current. It is evident from this plot that the simulated discharge current oscillates at a well-defined lower frequency with a higher beat on top. Moreover, the amplitude of oscillations appears to be stable. This illustrates how the data-driven closure model is capable of yielding convergent, time-resolved simulations–a critical capability given that Hall thrusters are known to oscillate for nearly all operating conditions. With that said, the average simulated result underpredicts the average measured current (8.5 A as opposed to 15 A), and the oscillation amplitude is higher in the simulation with a higher frequency compared to the experiment. We quantify these differences explicitly with the overlaid power spectral densities shown in Fig. Fig. 5(b). We note in this plot that the resolution of the experimental plot is higher than the simulated result as the experimental data was collected over a longer period than the simulation.

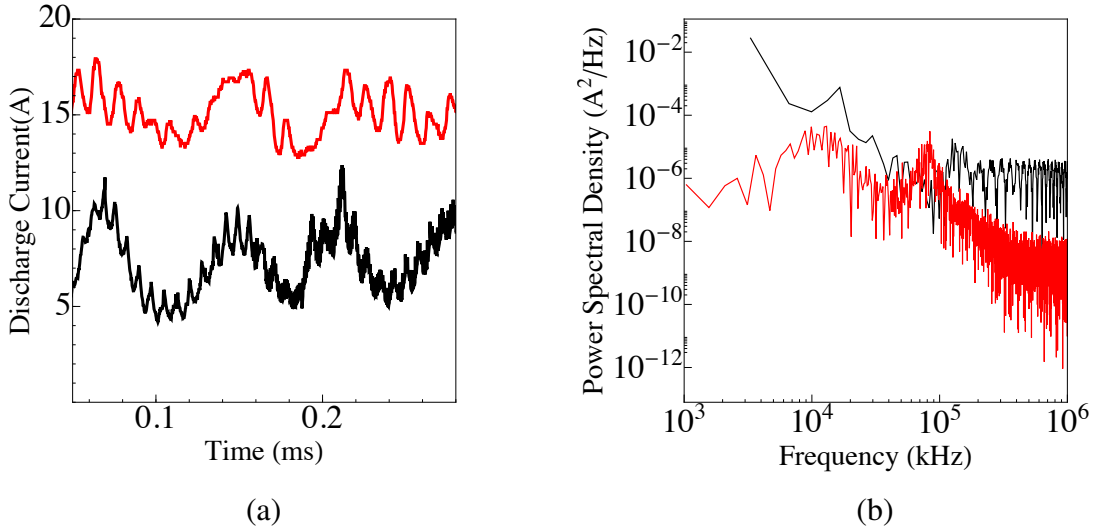

Fig. 5 a) Comparison of discharge current from simulation (black) and experiment (red). b) Power spectral densities of the two current traces. The simulation model parameters are $\Theta = (-0.071, 2.68, 3.42)$.

We compare in Fig. 6 the time-averaged ion velocity profiles on centerline as predicted from the Hall2De simulation and as measured in experiment. The positions have been normalized by the channel length, L, and are referenced with respect to the thruster anode ($z = 0$). In both cases, we again see qualitative similarities in the prediction and experiment. The ion velocity is characterized by a rapid acceleration near the exit plane of the thruster, culminating in a speed (and therefore kinetic energy) commensurate with the applied voltage, $V_d = 300$ V. With that said, the results with the data-driven closure show a more relaxed acceleration profile than the experimental result upstream of the exit plane ($z/L = 1$). As the steepness of the acceleration is directly a function of the electric field magnitude, this difference suggests the field in the simulated result is more spatially drawn out than in the experiment. We discuss the implications of this in the context of our other results in Sec. IV.

The large scale oscillations in the global discharge current predicted by simulation may be an indication that the local plasma properties in the thruster also vary in time. To illustrate this, we show in Fig. 7 the ion velocity profile at four different times during a simulated oscillation cycle. These are denoted by relative phases with respect to the first anti-node in the cycle ($0°, 90°, 180°, 270°$). This result shows the acceleration zone of the thruster, as characterized by

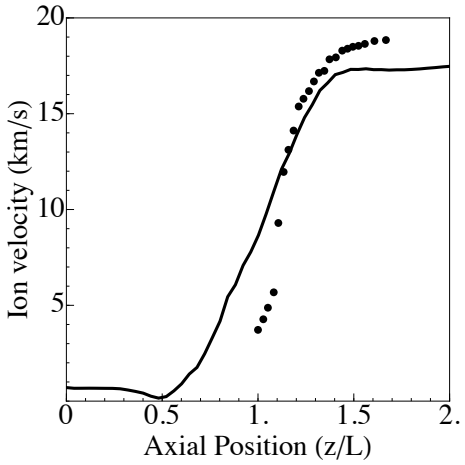

Fig. 6 Model predictions for ion velocity along channel centerline showing (black line) compared to experimental measurements (markers). Positions have been normalized to channel length, L, and are referenced with respect to the thruster anode at $z = 0$. The simulation model parameters are $\Theta = (-0.071, 2.68, 3.42)$

the location of most rapid increase in velocity, moving spatially with time by 10% of the discharge length. This type of movement of the plasma discharge has been measured before experimentally [45–49] and has been noted as a potential contributor to enhanced pole erosion in these devices [19]. The data-driven closure model incorporated into Hall2De appears to self-consistently capture this process.

With that said, while the preceding results serve to illustrate the capability of the data-driven closure to converge and yield physically plausible (if not validated) results, they only represent the predictions for one set of model parameters. As we discussed in Sec.III.A, there is inherent uncertainty in these parameters, which should be reflected in our model predictions. To this end, we consider in the next section the impact of propagating forward these uncertainties to the code's predictions.

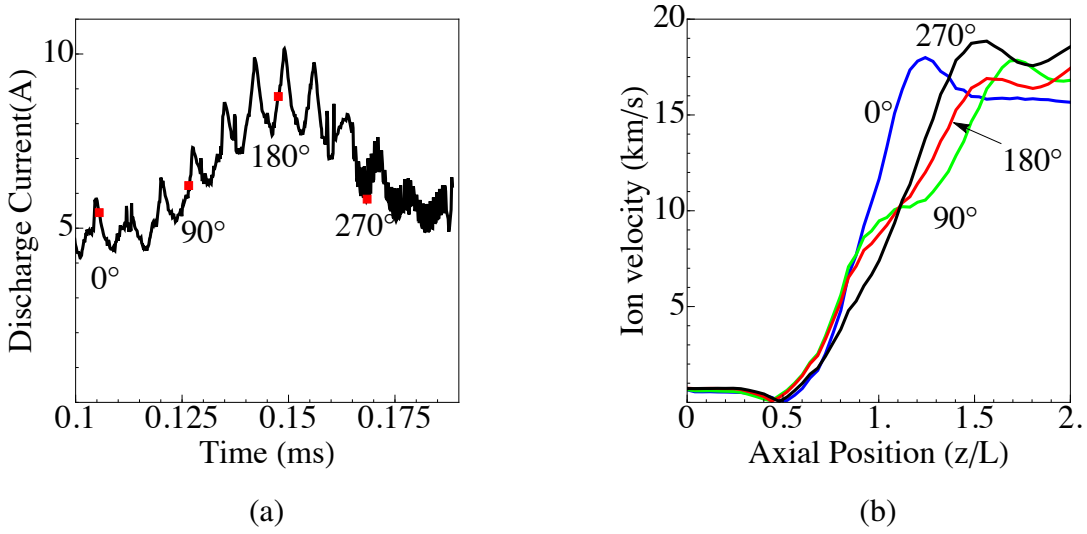

Fig. 7 a) Simulated discharge current for one cycle of the lower frequency oscillation with labeled phases. b) The ion velocity from the code output at the corresponding phases from (a). The simulation model parameters are $\Theta = (-0.071, 2.68, 3.42)$.

2. Probabilistic results

We consider here the impact of the uncertainty in the model parameters of Eq. 3 on the predictions of Hall2De. To this end, we used the same MCMC procedure described in Sec. III.A to sample 20 times from the posterior and ran the Hall2De simulation for each set of model parameters for a total time of 0.3 ms. From the predictions yielded by these 20 turns, we generated statistical assessments of the predicted discharge current, ion velocity, and performance metrics. We note that the number of samples was constrained by computational resources, and the reported set is too sparse to represent the true distribution of model outputs. We attempt to compensate for this in the following by applying smooth kernel distributions (Sec. III.A) to the samples.

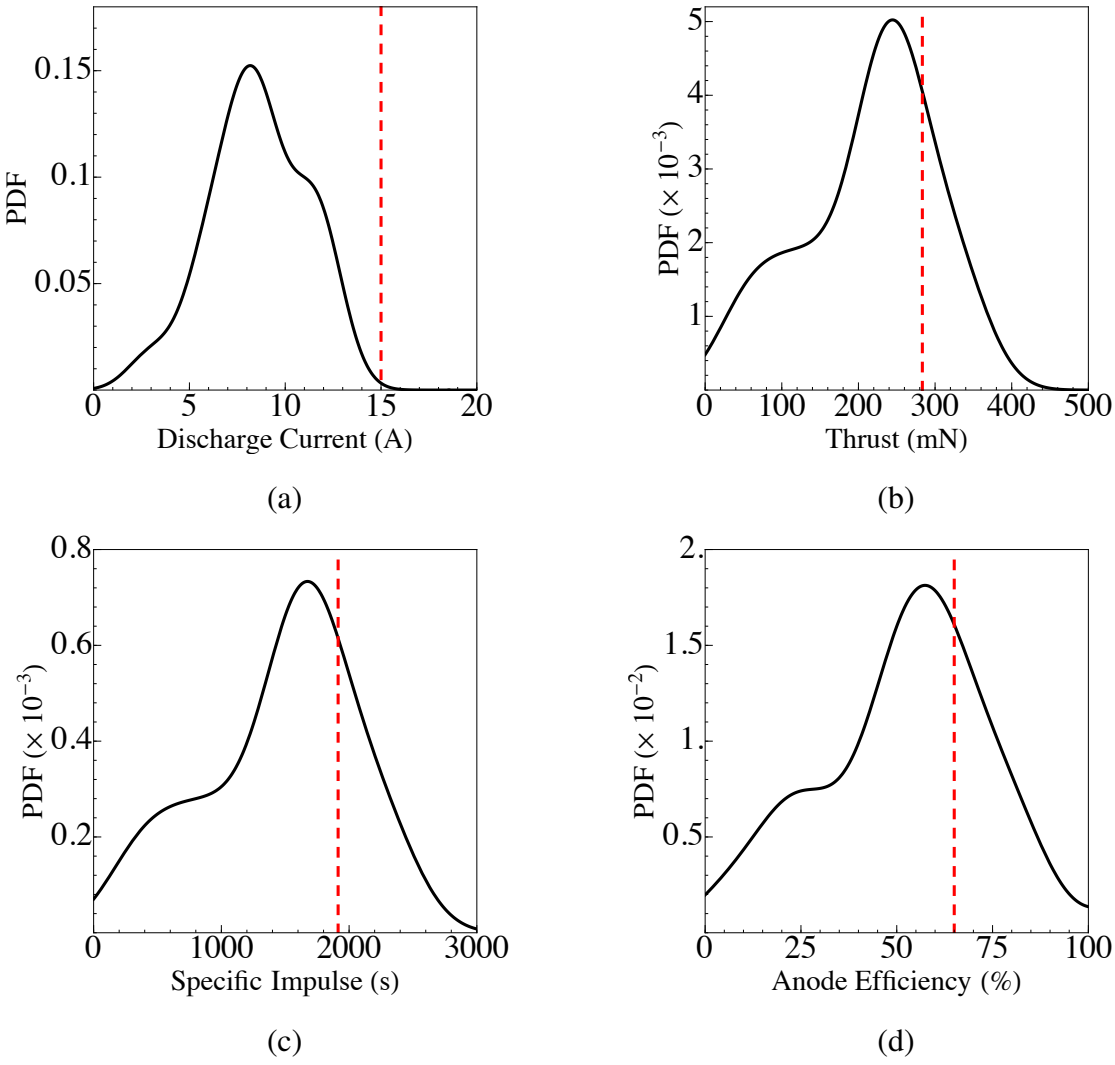

Fig. 8 Probability distribution functions of model predictions for the (a) average discharge current, (b) thrust, (c) specific impulse, and (d) anode efficiency. The experimentally measured values are denoted by vertical dashed lines.

With this in mind, we show in Fig. 8 the simulated probability distributions for average discharge current, thrust, specific impulse and anode efficiency. For comparison, we also show the experimentally-measured values (from Ref. [41, 42]) as vertical dashed lines. The discharge current result (Fig. 8(a)), illustrates two key features. First, there is a wide variance in the predicted distribution. This variance reflects the sensitivity of the code to the uncertainty in the model parameters and the sparsity of the sampling dataset. Second, reinforcing our finding from the single case study in Sec. III.B.1, this result shows that the median predicted current (I_D = 8.5 A) is lower than the experimental measurement (I_D = 15 A). There is a finite probability (the tail of the distribution) that the predicted current will be

15 A, but this probability is low—only approximately 5% confidence in this result. The performance metrics (Figs. 8c-d) exhibit the same two key features as the discharge current plots. In all cases the width of the distributions is large, leading to a low level of confidence in the model prediction. The experimentally measured values are close—albeit lower—compared to the most probable values for all of the distributions.

While most of the modeled cases showed stable, repeatable oscillations, the frequency and amplitude of oscillations varied depending on the model parameters. There were also some cases where the discharge current oscillations were quiescent . To capture these trends probabilistically, we show in Fig. 9(a) the distribution of the power spectra of the oscillations. We generated these results by performing a power spectral analysis on the time-dependent discharge currents for each simulation result. At each frequency value, we then estimated the median of the datasets (solid line) as well as the 5% and 95% confidence intervals (dashed lines) from the 20 samples. The shaded region therefore encapsulates 90% of the outputs from the reported samples. We also show for comparison the power spectral density from the experimental data.

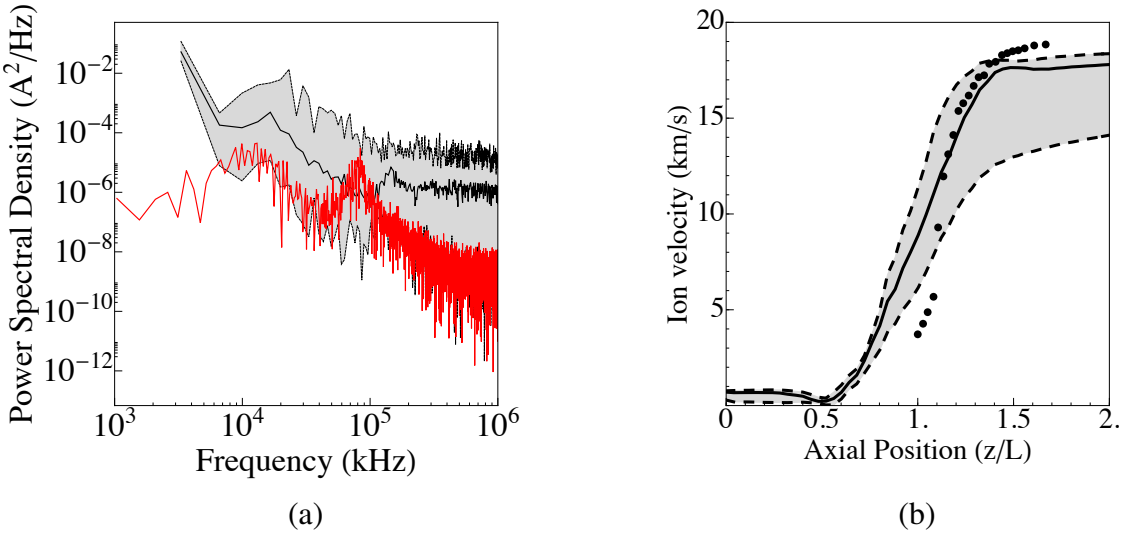

Fig. 9 a) Model predictions for power spectral density of discharge current showing the median (black line) and 5% and 95% confidence intervals (dashed line). The experimental measurement is denoted as a red line. b) Model predictions for ion velocity along channel centerline showing the median result (black line) and 5% and 95% confidence intervals (dashed line). Experimental measurements are indicated by black markers. Positions have been normalized to channel length, L, and are referenced with respect to the anode at $z = 0$.

The results in Fig. 9(a) show that on average the simulations predict an oscillation at ~ 18kHz, though the variance on this prediction captures the fact that some model results show quiescent operation. We also see on average the power spectra exhibits a higher frequency peak at ~ 100 kHz. This oscillation was evident in the single parameter simulation case in Fig. 5 and appears here to be a common feature over the sampled space. By comparison, the magnitude of the experimental spectra is lower— which is a direct indication that the experimental state is more quiescent than the simulated one. The experiment does show similar oscillatory features compared to the simulation, i.e. two difference types of oscillations; however, the frequencies of these are lower than the modeled result (12 kHz and 80 kHz).

We show in Fig. 9(b) the distribution of predictions for the average ion velocity along centerline compared to the experimental measurement. In this case, at each spatial location we calculated the median (solid line) and 5% and 95% confidence intervals (dashed lines) from the 20 samples. The shaded region therefore represents the predictions of 90% of the models. As can be seen, the median profile follows the shape as in Fig. 6; however, there is a marked degree of variance in the predictions. This results in uncertainties in the downstream ion velocities of 7.5 km/s. This relatively large variance underscores the sensitivity of the model outputs to the data-driven model parameters. We also note that while some of the experimental data does fall within the model predictions in the acceleration zone ($z/L = 1$), the predicted ion acceleration is on average more relaxed than indicated by experiment. This suggests that in aggregate the simulated results are systematically predicting ion acceleration that is too gradual.

IV. Discussion

The model results we presented in the preceding section are predictive in the sense that they did not require experimental measurements of the thruster performance or plasma properties to guide the model. Indeed, although we used a closure model that was discovered through symbolic regression of data, this dataset did not include the thruster configuration we have simulated here. As a promising preliminary result, we have found the model predictions are physically plausible. Though, the model predictions are not quantitatively consistent with experimental measurement. We discuss our results in the following in the context of the physical implications of the predicted trends, the limitations of our approach, and strategies for improving this technique.

A. Physical implications of modeling results with data-driven closure

The fact that our simulation result can predict a breathing mode-like oscillation is physically significant. The breathing mode, though ubiquitous in Hall thrusters, remains poorly understood. And while it is commonly accepted that this oscillation is a natural, ionization-based mode of the plasma, it is an open question as to what drives this mode unstable. One possibility that recently has been suggested is that it is necessary for some sort of feedback mechanism between electron transport in the downstream region and neutrals and ions in the upstream in order for this mode to grow [50]. While this type of feedback mechanism may not be captured by some closure models, an enabling feature of our approach is that the anomalous collision frequency (and therefore transport) of the electrons does self-consistently depend on the local plasma properties. This suggests the collision transport can be perturbed and respond to variations in the plasma properties, thus providing a feedback loop for growth.

Relatedly, the fact that the model predicts a second and higher frequency oscillation at $\sim$ 100 kHz that is qualitatively consistent with experiment is also of particular physical significance. The nature of this higher frequency oscillation in the discharge current in experimental measurements remains an open question. It is notable, however, that while this frequency has been attributed to a cathode borne, rotational mode [51], the fact that some content appears at this frequency in this r-z simulation suggests some other longitudinal mechanism may be responsible.

B. Limitations of data-driven method

Despite the qualitative agreement with experiment, the simulations with the data-driven closure still do not predict accurately the quantitative measurements of the plasma. For example, the ion acceleration in the simulation begins inside the channel at $z/L = 0.5$ and increases until $z/L = 1.5$ while the acceleration in experiment is more spatially condensed from $z/L = 1$ to $z/L = 1.5$. This suggests that the electric field—the field that accelerates the ions—is more spatially relaxed in the simulation than in the experiment. As the magnitude of the electric field is directly tied to the collisions (Eq. 1), this result may indicate that the anomalous collision frequency from the data-driven closure is too low in the upstream region. This is consistent with the results reported in Ref. [10] where it was remarked that the data-driven models generally did not perform as well in matching training data in the region upstream of the thruster acceleration zone.

Fig. 8 shows that the simulation underpredicts performance in terms of thrust, specific impulse, and efficiency. In light of the lower predicted current, these lower performance results suggest that the simulation may have too low an ionization fraction. As with the relaxed ion velocity profile, this low ionization fraction may in part be attributed to the relaxed electric field in the simulation. Since the electrons in the discharge are energized by Ohmic heating, a relaxed electric field as we see in the simulation will translate to lower effective electron temperatures and therefore reduced ionization.

In addition to the inability of the model to match experiment in our particular case study, there may be more fundamental limitations with applying a data-driven approach. Indeed, as was pointed in Ref. [10], even if a data-driven closure does accurately predict one new experimental condition, there is no guarantee that the model will be extensible to other operating points or thrusters. Similarly, as the transport process is inherently a kinetic effect, there is the possibility that fluid-based closures may never be able to fully predict the consequences of anomalous transport. Rigorous uncertainty quantification as we have employed here can be a mitigating factor for this latter possibility. We have demonstrated in this work the ability to encode our uncertainty in these closure models and in turn to directly quantify how this uncertainty impacts our confidence in the model predictions.

As a final caveat, we note that the statistics we have generated for model outputs in this work are based on a sparse dataset with only 20 entries. This stems from the limited computational resources at our disposal for this initial study. With an increased number of samples, the confidence intervals and median predictions will change, converging on the true probability distribution for model predictions. This does not ultimately mean that the variance will be reduced, but

the revised distributions will better reflect the impact of closure model uncertainty in the simulation results.

C. Strategies for improving model fidelity

While there are limitations to the approach we have applied, there are multiple methods through which we may improve model fidelity. As noted in the preceding section, the data-driven closure we have adopted does not accurately predict all of the relevant physical processes in the thruster. However, while we only focused on one model (Eq. 3) for this work, in Ref. [10] we identified hundreds of possible models (explicitly providing symbolic forms for three). These other closures may yield improved agreement with data, or alternatively, combining these data-driven models and sampling from each probabilistically may yield more accurate predictions.

With that said, ideally we would be able to replace a data-driven closure with a validated physics-based model. As we remarked in Ref. [10], the challenge with this approach stems from the fact that most physics-based closures proposed to date show lower fidelity compared to the data-driven models we have identified. However, these previous closures primarily have been treated as deterministic with fixed model parameters. A probabilistic approach combined with model inference may improve their fidelity–or at least help quantify the consequences of model uncertainty in these closures. In parallel, there are on-going efforts to derive higher fidelity physics-based closures (c.f. [33]) which also can be examined through a probabilistic approach.

D. Practical implications for engineering applications

As a last note, we remark that the ability to rigorously quantify uncertainty in Hall thruster model predictions will be a critical tool for future engineering applications of these models. In order to leverage these models to help address practical challenges such as quantifying the impact of ground tests on thruster operation or to perform lifetime risk assessment, there is a need to understand the sources of uncertainty in the models and their implications for model predictions. As we have discussed in the preceding, the challenge for Hall thruster modeling ultimately stems from how to quantify model uncertainty that stems from an incomplete understanding of key physical processes like the electron transport. The work we have presented here represents an initial attempt to assess this uncertainty and its consequences.

V. Conclusion

Ultimately, the results of this work stand apart from previous studies in two key ways. First, we have self-consistently incorporated a data-driven closure model for electron transport with a full thruster code and shown that it will yield physically realistic results. Second, we have demonstrated the ability to quantify how our uncertainty about the closure (and by extension the underlying physics of the thruster) impacts the predictions of a high-fidelity thruster model. This is a critical step for future practical applications of modeling efforts such as lifetime qualification and optimal design where there is a need to understand the confidence in model predictions and the associated risks with these predictions.

VI. Acknowledgements

This work was supported by an AFOSR award (FA9550-19-1-0022) under the Space Propulsion and Power portfolio. The authors also would like to acknowledge the creator of Hall2De, Dr. Ioannis Mikellides, of the California Institute of Technology's Jet Propulsion Laboratory, for providing an executable copy of the model. The authors similarly would like to thank Dr. Alejandro Lopez Ortega, also of JPL, for his assistance with Hall2De.

References

[1] Byers, D., and Dankanich, J., "A Review of Facility Effects on Hall Effect Thrusters," *Presented at the 31st International Electric Propulsion Conference, IEPC-2009-076*, 2009.

[2] Dankanich, J. W., Walker, M., Swiatek, M. W., and Yim, J. T., "Recommended practice for pressure measurement and calculation of effective pumping speed in electric propulsion testing," *Journal of Propulsion and Power*, Vol. 33, No. 3, 2017, pp. 668–680.

[3] Byrne, M. P., Jorns, B. A., and Arbor, A., "Data-driven Models for the Effects of Background Pressure on the Operation of Hall Thrusters," *Presented at the 36th International Electric Propulsion Conference, Vienna Austria, IEPC–2019–630*, 2019.

[4] Brophy, J., Polk, J., Randolph, T., and Dankanich, J., "Lifetime Qualification Standards for Electric Thrusters for Deep-Space Missions," *44th AIAA Joint Propulsion Conference and Exhibit*, 2008, pp. AIAA–2008–5184.

[5] Herman, D., Tofil, T., Santiago, W., Kamhawi, H., Polk, J., Snyder, J. S., Hofer, R., Picha, F., and Schmidt, G., "Overview of the development of the advanced electric propulsion system (AEPS)," *Proceedings of the 35th International Electric Propulsion Conference, Atlanta, GA, IEPC-2017-284*, 2017.

[6] Oh, D., "Development of the Psyche Mission for NASA's Discovery Program," *35th International Electric Propulsion Conference, Atlanta, GA, IEPC–2017–153*, 2017.

[7] Boeuf, J.-P., "Tutorial: Physics and Modeling of Hall Thrusters," *Journal of Applied Physics*, Vol. 121, No. 1, 2017, p. 011101. https://doi.org/10.1063/1.4972269.

[8] Mikellides, I. G., and Ortega, A. L., "Challenges in the development and verification of first-principles models in Hall-effect thruster simulations that are based on anomalous resistivity and generalized Ohm's law," *Plasma Sources Science and Technology*, Vol. 28, No. 1, 2019, p. 014003.

[9] Taccogna, F., and Garrigues, L., "Latest progress in Hall thrusters plasma modelling," *Reviews of Modern Plasma Physics*, Vol. 3, No. 1, 2019.

[10] Jorns, B., "Predictive, data-driven model for the anomalous electron collision frequency in a Hall effect thruster," *Plasma Sources Science and Technology*, Vol. 27, No. 10, 2018.

[11] Mikellides, I. G., and Katz, I., "Numerical Simulations of Hall-effect Plasma Accelerators on a Magnetic-Field-Aligned Mesh," *Physical Review E*, Vol. 86, No. 4, 2012, pp. 1–17.

[12] Hagelaar, G. J. M., Bareilles, J., Garrigues, L., and Boeuf, J. P., "Role of anomalous electron transport in a stationary plasma thruster simulation," *Journal of Applied Physics*, Vol. 93, No. 1, 2003, pp. 67–75.

[13] Hofer, R., Katz, I., Mikellides, I., Goebel, D. M., Jameson, K. K., Sullivan, R. M., and Johnson, L. K., "Efficacy of Electron Mobility Models in Hybrid-PIC Hall Thruster Simulations," *Proceedings of the 44th AIAA Joint Propulsion Conference*, 2008.

[14] Escobar, D., and Ahedo, E., "Low-frequency azimuthal stability analysis of Hall thrusters," *AIAA Joint Propulsion Conference*, , No. 2012-4180, 2012. https://doi.org/doi:10.2514/6.2012-4180.

[15] Hara, K., Sekerak, M. J., Boyd, I. D., and Gallimore, A. D., "Mode transition of a Hall thruster discharge plasma," *Journal of Applied Physics*, Vol. 115, No. 20, 2014.

[16] Mikellides, I. G., Jorns, B., Katz, I., and Ortega, A. L., *Hall2De Simulations with a First-principles Electron Transport Model Based on the Electron Cyclotron Drift Instability*, AIAA-2016-4618, 2016.

[17] Lopez Ortega, A., Mikellides, I., and Chaplin, V., "Numerical Simulations for the Assessment of Erosion in the 12.5-kW Hall Effect Rocket with Magnetic Shielding (HERMeS)," *Proceedings of the 35th International Electric Propulsion Conference, Atlanta, GA, IEPC-2017-154*, 2017.

[18] Smolyakov, A. I., Chapurin, O., Frias, W., Koshkarov, O., Romadanov, I., Tang, T., Umansky, M., Raitses, Y., Kaganovich, I. D., and Lakhin, V. P., "Fluid theory and simulations of instabilities, turbulent transport and coherent structures in partially-magnetized plasmas of E × B discharges," *Plasma Physics and Controlled Fusion*, Vol. 59, No. 1, 2017. https://doi.org/10.1088/0741-3335/59/1/014041.

[19] Lopez Ortega, A., and Mikellides, I. G., "Investigations of Pole Erosion Mechanisms in the 12.5 kW HERMeS Hall Thruster with the Hall2De Code," *2018 Joint Propulsion Conference*, 2018.

[20] Mikellides, I. G., Katz, I., Hofer, R. R., Goebel, D. M., de Grys, K., and Mathers, A., "Magnetic shielding of the channel walls in a Hall plasma accelerator," *Physics of Plasmas*, Vol. 18, No. 3, 2011, p. 033501. https://doi.org/10.1063/1.3551583, URL https://doi.org/10.1063/1.3551583.

[21] Mikellides, I. G., Katz, I., Hofer, R. R., and Goebel, D. M., "Magnetic shielding of a laboratory Hall thruster. I. Theory and validation," *Journal of Applied Physics*, Vol. 115, No. 4, 2014, pp. 0–20. https://doi.org/10.1063/1.4862313.

[22] Lopez Ortega, A., Mikellides, I. G., Chaplin, V. H., Snyder, J. S., and Lenguito, G., "Facility pressure effects on a Hall thruster with an external cathode, I: Numerical simulations," *Plasma Sources Science and Technology*, Vol. 29, No. 3, 2020. https://doi.org/10.1088/1361-6595/ab6c7f.

[23] Mikellides, I. G., Ortega, A. L., Chaplin, V. H., and Snyder, J. S., "Facility pressure effects on a Hall thruster with an external cathode, II: Theoretical model of the thrust and the significance of azimuthal asymmetries in the cathode plasma," *Plasma Sources Science and Technology*, Vol. 29, No. 3, 2020. https://doi.org/10.1088/1361-6595/ab6c7f.

[24] Fife, J. M., and Martinez-Sanchez, M., "Two-Dimensional Hybrid Particle-in-Cell (PIC) Modeling of Hall Thrusters," *Proceedings of the 24th International Electric Propulsion Conference*, 1995.

[25] Morozov, A. I., and Savelyev, V. V., *Fundamentals of Stationary Plasma Thruster Theory*, Springer US, Boston, MA, 2000, pp. 203–391. https://doi.org/10.1007/978-1-4615-4309-1_2, URL https://doi.org/10.1007/978-1-4615-4309-1{_}2.

[26] Barral, S., Makowski, K., PeradzyÅski, Z., Gascon, N., and Dudeck, M., "Wall material effects in stationary plasma thrusters. II. Near-wall and in-wall conductivity," *Physics of Plasmas*, Vol. 10, No. 10, 2003, pp. 4137–4152. https://doi.org/10.1063/1.1611881.

[27] Garrigues, L., Hagelaar, G. J., Boniface, C., and Boeuf, J. P., "Anomalous conductivity and secondary electron emission in Hall effect thrusters," *Journal of Applied Physics*, Vol. 100, No. 12, 2006. https://doi.org/10.1063/1.2401773.

[28] Scharfe, M. K., Thomas, C. A., Scharfe, D. B., Gascon, N., Cappelli, M. A., and Fernandez, E., "Shear-Based Model for Electron Transport in Hybrid Hall Thruster Simulations," *IEEE Transactions on Plasma Science*, Vol. 36, No. 5, 2008, pp. 2058–2068.

[29] Katz, I., Mikellides, I. G., Jorns, B. a., and Ortega, A. L., "Hall2De Simulations with an Anomalous Transport Model," *Proceedings of the 34th International Electric Propulsion Conference,IEPC-2015-402*, 2015.

[30] Cappelli, M. A., Young, C. V., Cha, E., and Fernandez, E., "A zero-equation turbulence model for two-dimensional hybrid Hall thruster simulations," *Physics of Plasmas*, Vol. 22, No. 11, 2015, p. 114505. https://doi.org/10.1063/1.4935891.

[31] Lafleur, T., Baalrud, S. D., and Chabert, P., "Theory for the anomalous electron transport in Hall effect thrusters. II. Kinetic model," *Physics of Plasmas*, Vol. 23, No. 5, 2016, p. 053503. https://doi.org/10.1063/1.4948496.

[32] Lafleur, T., Baalrud, S. D., and Chabert, P., "Theory for the anomalous electron transport in Hall effect thrusters. I. Insights from particle-in-cell simulations," *Physics of Plasmas*, Vol. 23, No. 5, 2016, p. 053502. https://doi.org/10.1063/1.4948495.

[33] Jorns, B., "Two Equation Closure Model for Plasma Turbulence in a Hall Effect Thruster," *36th International Electric Propulsion Conference, Vienna, Austria*, 2019, pp. IEPC–2019–129.

[34] Goebel, D. M., and Katz, I., *Fundamentals of Electric Propulsion: Ion and Hall Thrusters*, JPL Space Science and Technology Series, 2008.

[35] Gelman, A., Carlin, J., Stern, H., Dunson, D., Vehtari, A., and Rubin, D., *Bayesian Data Analysis, Third Edition*, Chapman & Hall/CRC Texts in Statistical Science, Taylor & Francis, 2013.

[36] Robert, C., and Casella, G., *Monte Carlo Statistical Methods*, Springer, 2010.

[37] Jorns, B., Hofer, R., and Mikellides, I., "Power dependence of the electron anomalous collision frequency in a Hall thruster," *50th AIAA/ASME/SAE/ASEE Joint Propulsion Conference 2014*, 2014. https://doi.org/10.2514/6.2014-3620.

[38] Conversano, R. W., Goebel, D. M., Hofer, R. R., Mikellides, I. G., Katz, I., and Wirz, R. E., "Magnetically Shielded Miniature Hall Thruster: Design Improvement and Performance Analysis," 2015, pp. 1–12.

[39] Mikellides, I. G., and Lopez Ortega, A., "Numerical Simulations of a 100-kW Class Nested Hall Thruster with the 2-D Axisymmetric Code Hall2De," *35th International Electric Propulsion Conference, Atlanta, GA,IEPC–2017–220*, 2017.

[40] Hofer, R., Cusson, S., Lobbia, R., and Gallimore, A., "The H9 Magnetically Shielded Hall Thruster," *Proceedings of the 35th International Electric Propulsion Conference*, 2017.

[41] Cusson, S. E., Hofer, R., Lobbia, R., Jorns, B., and Gallimore, A., "Performance of the H9 Magnetically Shielded Hall Thrusters," *Proceedings of the 35th International Electric Propulsion Conference*, 2017.

[42] Cusson, S. E., "Impact of Neutral Density on the Operation of High-Power Magnetically Shielded Hall Thrusters," *Phd Thesis, University of Michigan*, 2019.

[43] Cusson, S. E., Dale, E. T., Jorns, B. A., and Gallimore, A. D., "Acceleration Region Dynamics in a Magnetically Shielded Hall Thruster," *Physics of Plasmas*, Vol. 26, No. 023506, 2019. https://doi.org/10.1063/1.5079414.

[44] Silverman, B., *Density Estimation for Statistics and Data Analysis.*, London: Chapman & Hall/CRC, 1986.

[45] Mazouffre, S., Gawron, D., and Sadeghi, N., "A time-resolved laser induced fluorescence study on the ion velocity distribution function in a Hall thruster after a fast current disruption," *Physics of Plasmas*, Vol. 16, No. 4, 2009, p. 43504.

[46] Durot, C. J., Gallimore, A. D., and Smith, T. B., "Validation and Evaluation of a Novel Time-Resolved Laser-Induced Fluorescence Technique," *Review of Scientific Instruments*, Vol. 85, No. 1, 2014, pp. 1–14. https://doi.org/10.1063/1.4856635.

[47] MacDonald, N. a., Cappelli, M. a., and Hargus, W. a., "Time-synchronized continuous wave laser-induced fluorescence axial velocity measurements in a diverging cusped field thruster," *Journal of Physics D: Applied Physics*, Vol. 47, No. 11, 2014, p. 115204.

[48] Dale, E. T., and Jorns, B., "Non-Invasive Time-Resolved Measurements of Anomalous Collision Frequency in a Hall Thruster," *Physics of Plasmas*, Vol. 26, No. 013516, 2019. https://doi.org/10.1063/1.5077008.

[49] Chaplin, V. H., Lobbia, R. B., Lopez Ortega, A., Mikellides, I. G., Hofer, R. R., Polk, J. E., and Friss, A. J., "Time-resolved ion velocity measurements in a high-power Hall thruster using laser-induced fluorescence with transfer function averaging," *Applied Physics Letters*, Vol. 116, No. 23, 2020, p. 234107. https://doi.org/10.1063/5.0007161.

[50] Dale, E. T., and Jorns, B. A., "Two-zone Hall thruster breathing mode mechanism, Part II: Experiment," *36th International Electric Propulsion Conference*, 2019, pp. 1–14.

[51] Jorns, B. A., and Hofer, R. R., "Plasma oscillations in a 6-kW magnetically shielded Hall thruster," *Physics of Plasmas*, Vol. 21, No. 5, 2014. https://doi.org/10.1063/1.4879819, URL http://dx.doi.org/10.1063/1.4879819.